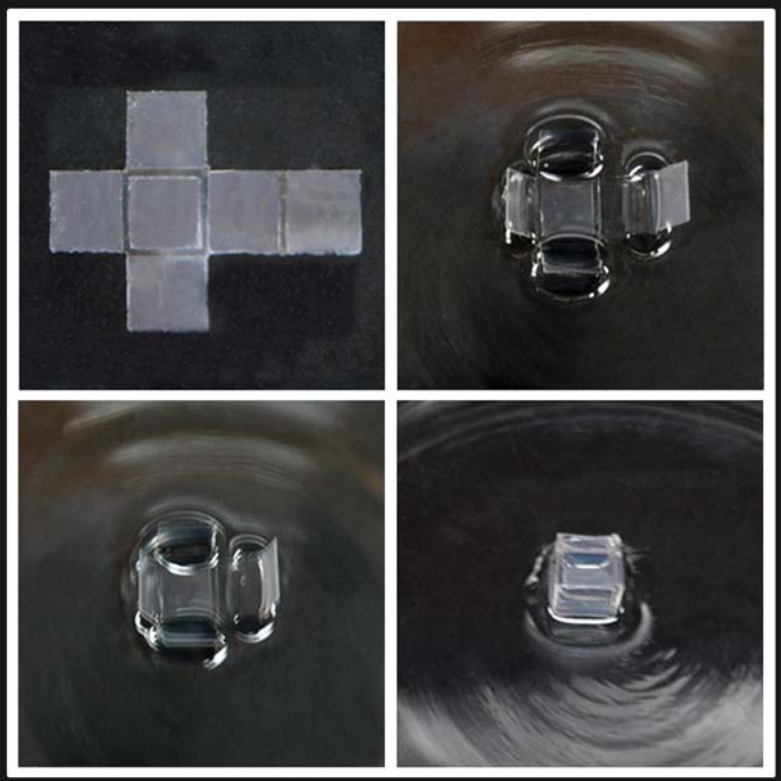

Showcasing collaborative research from K.-U. Jeong (Chonbuk National University), J.-H. Jang (UNIST), S. Z. D. Cheng (University of Akron), and E. L. Thomas (MIT) labs.

Title: Three-dimensional actuators transformed from the programmed two-dimensional structures *via* bending, twisting and folding mechanisms

Reversible colour and shape tunable photonic actuators were constructed by transforming the programmed 2D structures to the 3D objects via bending, twisting and folding mechanisms. Combined with the lithographic patterning technology, this unique technique may have a great potential for the applications in mechanical actuators and bio-mimetic devices.

As featured in:

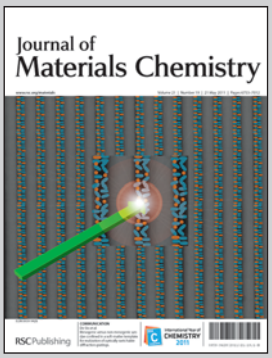

See Jeong *et al.*, *J. Mater. Chem.*, 2011, **21**, 6824.

RSC Publishing

www.rsc.org/materials

Registered Charity Number 207890

Journal of Materials Chemistry

Dynamic Article Links

Cite this: *J. Mater. Chem.*, 2011, **21**, 6824

www.rsc.org/materials

PAPER

Three-dimensional actuators transformed from the programmed two-dimensional structures *via* bending, twisting and folding mechanisms

Kwang-Un Jeong,*[a] Ji-Hyun Jang,*[b] Dae-Yoon Kim,[a] Changwoon Nah,[a] Joong Hee Lee,[a] Myong-Hoon Lee,[a] Hao-Jan Sun,[c] Chien-Lung Wang,[c] Stephen Z. D. Cheng[c] and Edwin L. Thomas[d]

Received 25th October 2010, Accepted 26th January 2011
DOI: 10.1039/c0jm03631e

Combining the physical principle of actuators with the basic concept of photonic crystals, colour-tunable three-dimensional (3D) photonic actuators were successfully fabricated. By controlling the *d*-spacings and the refractive index contrasts of the self-assembled 3D colloidal photonic crystals, colours of the photonic actuators were tuned. Various shapes of these 3D actuating objects were constructed by transforming the programmed 2D structures *via* bending, twisting and folding mechanisms. These 2D structures were first programmed by breaking the symmetry. The selective swellings were then applied as driving forces to control the shapes and colours of the photonic actuators. Scroll photonic actuators had been first demonstrated by bending the traditional 2D cantilever structure (K.-U. Jeong, *et al.*, *J. Mater. Chem.*, 2009, **19**, 1956). By breaking the symmetry of a cantilever structure perpendicular to its long axis, polypeptide-/DNA-like 3D helical photonic actuators were obtained from the programmed 2D structure *via* twisting processes. Both left- and right-handed scrolls and helices with various colours can be achieved by changing the polarity of solvents. Different types of 3D actuators, such as cube, pyramid and phlat ball, were also demonstrated *via* the folding mechanism. The reversible 3D photonic actuators transformed from the programmed 2D structures *via* the bending, twisting and folding mechanisms may be applied in the field of mechanical actuators, and optoelectronic and bio-mimetic devices.

Introduction

Constructions of three-dimensional (3D) objects with arbitrary shapes and further manipulations of their colours and shapes can provide many potential applications in the field of actuators, and bio-mimetic devices.[1,2] Various 3D structures have been fabricated by several sophisticated techniques including 3D printing and two-photon/interference lithography.[3,4] However, they are time consuming and cost-inefficient. Recently, smart materials have attracted much attention due to the ability to change their volume and shape in response to external stimuli.[5] If a 3D object can be obtained by folding, bending, and twisting a programmed 2D structure consisted of stimuli-responsive materials, we can construct smart 3D objects, which can reversibly change their shapes and properties. In addition, these methods are less expensive and easier to fabricate 3D structures compared with the traditional lithographic techniques.

Bending is an interesting and simple mode among inhomogeneous deformations from the viewpoint of applications of soft actuators.[6–9] Several research groups reported the bending deformation by creating the finite gradient of temperature or light intensity through the thickness of the films.[9] The bending behaviours are also observed at molecular dimensions, in which superstructures can be obtained *via* the assembly of two-component segmented building blocks.[10] Another example can be found in the formation of the scrolled polymer crystals rather than the conventional flat lamellar single crystals.[8] The curvature of the scrolled lamellae indicates that the inner and outer lamellar surfaces are unbalanced.[8]

Two of the most important geometric structures found in nature are the deoxyribonucleic acid (DNA) double helical structure and the polypeptide helical structure.[11] As it is known, DNA double helical structures contain information required for living cells to make the correct proteins for normal biological function. In addition to biology, helical structures have been intensively studied and developed in electro-optical materials science and technologies. Recently, Cheng and his coworkers have constructed double twisted structures from a series of

[a]*Department of Polymer-Nano Science and Technology, Department of BIN Fusion Technology, and Polymer Materials Fusion Research Centre, Chonbuk National University, Jeonju, 561-756, Korea. E-mail: kujeong@chonbuk.ac.kr; Fax: +82 63 270 2341; Tel: +82 63 270 4633*
[b]*Interdisciplinary School of Green Energy, Ulsan National Institute of Science and Technology, Ulsan, 689-798. E-mail: clau@unist.ac.kr*
[c]*Department of Polymer Science, The University of Akron, Akron, OH, 44325-3909, USA*
[d]*Institute for Soldier Nanotechnologies and Department of Materials Science and Engineering, Massachusetts Institute of Technology, Cambridge, MA, 02139, USA*

specifically designed main-chain non-racemic chiral polyesters.[5,12] In their system, the handedness of the helix is not only determined by the configurational chirality but also by the number of methylene groups in the repeat unit of the chiral polyesters. Additionally, helical structures from achiral molecules, such as achiral bent-core molecules and achiral biphenyl carboxyl acids have been constructed.[13] These researches reveal that the asymmetric structures are favourable to form twisted objects.

Another interesting instance of 3D objects with arbitrary shape is "origami" which can be realized *via* a paper folding process.[14] Gracias and his coworkers have shown that the assembled nanoscale panels jointed by metal hinges can transform to the polyhedral shape *via* the folding process.[15] However, it needs very tedious steps and contains metal hinges which might cause unexpected difficulties for the applications.[16]

Here, by combining the physical principle of actuators with the basic concept of photonic crystals, we demonstrate an easy way to fabricate reversible and colour-tunable photonic actuators responding to both hydrophilic and hydrophobic chemical environments through a symmetry breaking process and a change in the lattice constant of the photonic crystal structure. Scroll and helical photonic actuators can be constructed by transforming the programmed 2D structures *via* the bending and twisting processes, respectively. Both left- and right-handed scrolled and helical photonic actuators with various colours can be achieved by simply changing the polarity of solvents. Various 3D actuating objects, such as cube, pyramid and phlat ball, are also able to be constructed *via* the folding processes. The reversible 3D photonic actuators are successfully transformed from the programmed 2D structures *via* the bending, twisting and folding mechanisms.

Results and discussion

Our photonic actuators mainly consist of two layers of polymers firmly linked by covalent bonds. A thermally curable hydrophobic poly(dimethylsiloxane) (PDMS) and a UV-curable hydrophilic polyurethane (PU)/2-hydroxyethyl methacrylate (HEMA) elastomeric blending precursor are selected as constituents because of their flexibility, optical transparency and dramatically different swelling responses to selected solvents. The HEMA content in the hydrophilic PU/HEMA layer is optimized at 30 wt% which is determined from the experimental results of differential scanning calorimetry and dynamic mechanical analysis, combined with the requirement of mechanical properties.[1] As shown in schematic illustration in Fig. 1, colour-/shape-tunable photonic actuators, such as scroll, helical, and cubic actuators, can be fabricated through various processes.

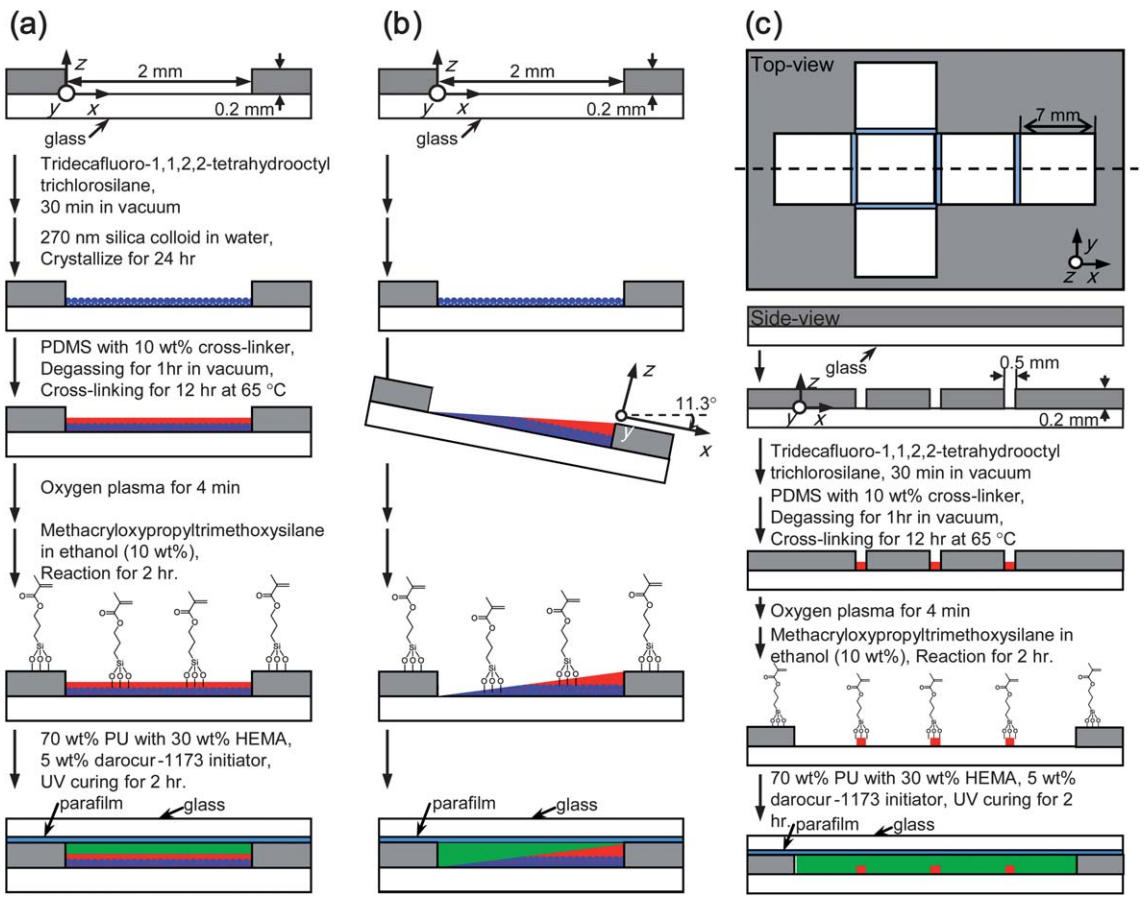

Fig. 1 Fabrication processes of colour-tunable actuators: (a) bending,[1] (b) twisting, and (c) folding techniques. Here, PDMS, PU/HEMA, and silica nanoparticles are represented in red, green and blue colours, respectively.

For the fabrication of scroll and helical photonic actuators, colloidal silica nanoparticles with a diameter of 270 nm are first self-assembled to a near single crystalline face-centred cubic (FCC) opal structure using Colvin's method. Note that a fluorinated silane monolayer is built on the surface of the mold before the self-assembly of photonic crystals for the purpose of an easy peel-off process. Scanning electron microscope (SEM) images of the assembled silica colloidal FCC structure on the [111] and [$0\bar{1}1$] zones are shown in Fig. 2a and b, respectively. When PDMS monomer with 10 wt% crosslinker is infiltrated into the silica FCC photonic crystal and cured at 65 °C for 12 h, the silica photonic crystal does not open any photonic band gap since the refractive index ($n \cong 1.43$) of PDMS is identical with that of silica nanoparticles. Therefore, the resulting PDMS/silica colloid composite layer is transparent. For the case of helical photonic actuators, before the PDMS infiltration process, the mold is tilted at a certain angle as shown in Fig. 1b in order to break symmetry on the *xz*-plane. Depending on the tilting angle, the twisting power of helical photonic actuator is able to be controlled. Before applying the second hydrophilic PU/HEMA layer, a self-assembled methacryloxypropyltrimethoxysilane monolayer on the PDMS is prepared on the oxygen plasma treated PDMS surface as shown in Fig. 1a and b. By exposing to UV lights for 2 h, PU70/HEMA30 is photo-polymerized and strong chemical bonds are also created between hydrophilic PU70/HEMA30 and hydrophobic PDMS layers. Here, parafilms and glass plates are placed on the top of the mold during the UV curing process to obtain an even sample thickness. Photographic images of the final transparent scroll and helical photonic actuators in the dry state are shown in Fig. 2c.

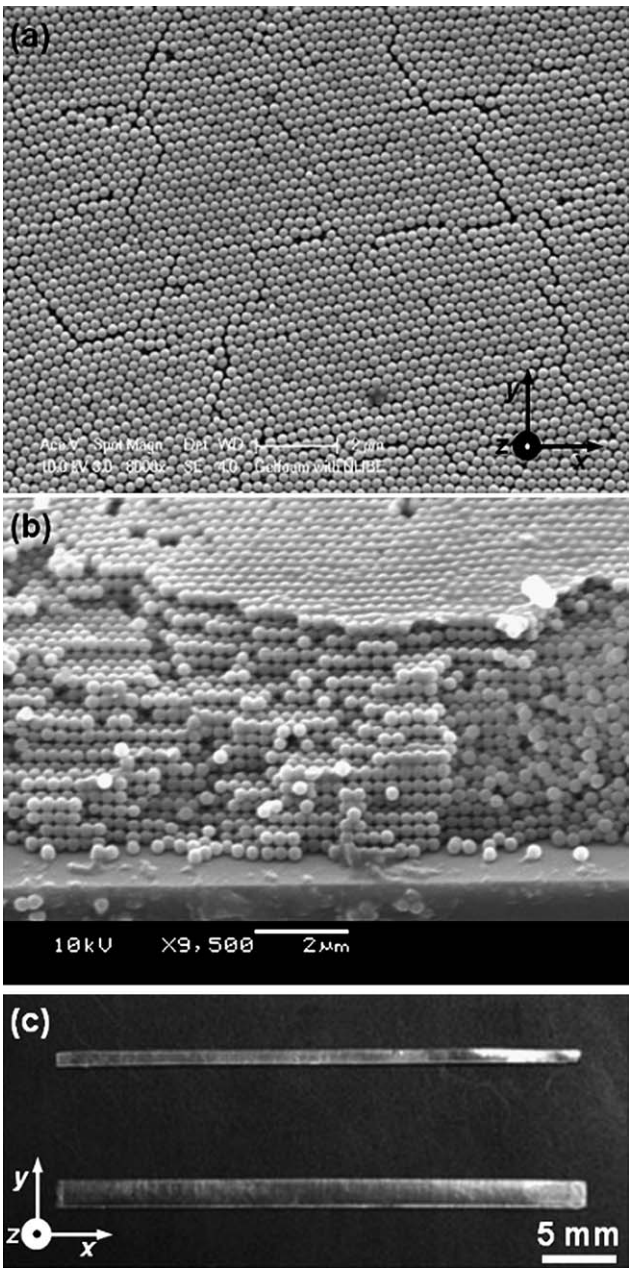

Fig. 2 SEM images of silica colloidal FCC structure: (a) [111] zone and (b) [$0\bar{1}1$] zone.[1,17] (c) is the photographic image of scroll and helical photonic actuators.

The swelling expansion ratio of the PDMS and PU70/HEMA30 layers are estimated in different solvents, such as hexane, acetic acid and ethyl acetate. The maximum swelling expansion ratio (V_{max}/V_0) of the hydrophobic PDMS layer is 2.28 in hexane and 1.10 in acetic acid. On the other hand, the V_{max}/V_0 of hydrophilic PU70/HEMA30 is 1.00 in hexane and 2.05 in acetic acid. Here, V represents the expanded volume before contacting with solvent at a certain swelling time (t) and V_0 is the initial volume at $t = t_0$. Both PDMS and PU70/HEMA30 layers are swollen more than 90% of their maximum swelling expansion ratio in the first 10 min of the contacting time. However, their deswelling processes take longer times than their swelling processes. The gel contents of the thermally cured PDMS and the UV-cured PU70/HEMA30 layers are also evaluated by the swelling weight ratio in good solvents. The gel contents of PDMS (in hexane) and PU70/HEMA30 (in acetic acid) are measured to be 100% and 99%, respectively. More detailed explanations of swelling and deswelling processes of PDMS and PU70/HEMA30 with respect to time and solvent have been previously reported in ref. 1.

Optical behaviours of the silica photonic crystals embedded in PDMS layer are also investigated. Since the diameter of a silica particle is 270 nm and its close packed crystal is FCC structure, 70% reflectivity at a wavelength of 590 nm is obtained along the [111] zone. This measurement is utilized by an optical microscope equipped with a fiber-optic spectrometer using a silver-coated metallic mirror as a 100% reference. When the transparent silica colloid/PDMS layer is swollen in a relatively poor solvent of PDMS, acetic acid, the spacings between silica nanoparticles expand and the refractive index contrast between silica nanoparticle and PDMS containing acetic acid solvent are increased. This leads to a red shift of reflection peak with its maximum intensity (~30%) centred at 659 nm. On the other hand, a broad and low intensity peak (~7%) at 459 nm is observed in a good solvent (hexane) along the [111] zone. More detailed descriptions of colour changes depending on solvents can be found in a previously reported communication.[1]

A cantilever is one of the simplest and the most frequently demonstrated actuating structures actuated by the bending mechanism. As shown in Fig. 1a and 3a, a cantilever can be fabricated by sandwiching two dramatically dissimilar planar

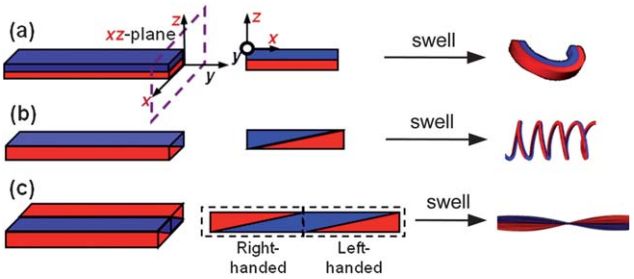

Fig. 3 Schematic illustrations of (a) bending, (b) polypeptide-type twisting, and (c) DNA-type twisting actuators.

structures differently responding to the external forces, such as solvent, pH, light, and electric/magnetic fields. Selective swelling triggers the actuation in this system by making one layer expand more drastically than the other. The unbalanced expansion between top and bottom layers results in a scrolled structure. Strong adhesion between two layers is achieved by creating covalent bonds between PDMS and PU70/HEMA30 layers in this system. Since the V_{max}/V_0 of the PDMS and PU70/HEMA30 layers in hydrophobic hexane corresponds to 2.28 and 1.00, respectively, a bluish left-handed scroll is formed in hydrophobic hexane solvent, as shown in Fig. 4a.[1] When the transparent cantilever is immersed in hydrophilic acetic acid solvent, a reddish right-handed scroll forms by a bending mechanism, as shown in Fig. 4b.[1] The scrolled photonic actuator returns back to a transparent planar structure when the acetic acid is completely evaporated, indicating that the switch is fully reversible without observable damages.

To fabricate 3D objects transformed from a programmed 2D surface by a twisting mechanism, the symmetry of bilayer planar structure on the *xz*-plane is broken, as schematically illustrated in Fig. 1b and 3b. The same materials as the ones working *via* bending mechanism, PDMS and PU/HEMA, are used. By making a sloped bilayer structure, the planar structure described in Fig. 3b can be bended along the *y*-axis as well as be twisted around this axis when one of the layers is asymmetrically expanded in a specifically selected solvent. When the bilayer actuating device with triangular PDMS and PU/HEMA layers with respect to the *y*-axis is swollen, a helical-type actuating sensor can be formed, as shown in Fig. 5. The detailed fabrication process for the helical photonic actuator is described in Fig. 1b. The size of the triangular PDMS region is one of the

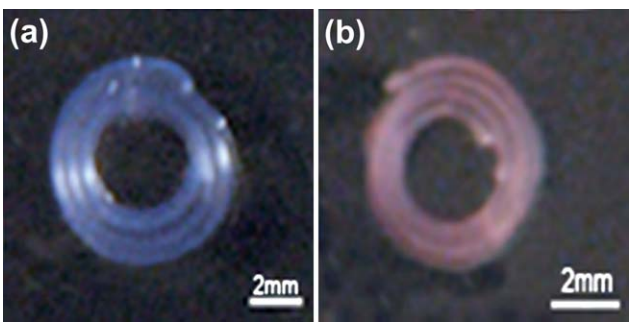

Fig. 4 Photographic images of (a) left-handed (after 70 s in hexane) and (b) right-handed (after 100 s in acetic acid) bending actuators.[1]

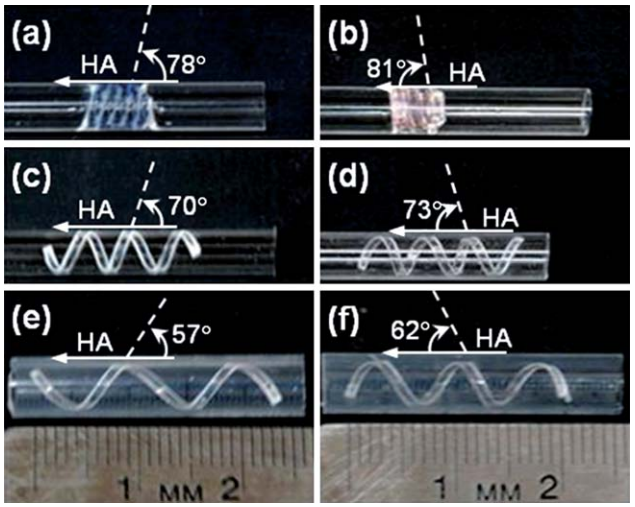

Fig. 5 Left-handed polypeptide-type twisting actuator (a) taken after 70 s in hexane and after drying the solvent in confined tubes: (c) 3.5 mm (taken after 5 min) and (e) 4.5 mm (taken after 20 min), respectively. Right-handed polypeptide-type twisting actuator (b) taken after 100 s in acetic acid and after drying the solvent in confined tubes: (d) 3.5 mm (taken after 4 min) and (f) 4.5 mm (taken after 25 min), respectively. HA refers to helical axis.

main factors determining the twisting power of the helical actuating sensor. A left-handed helix with a bluish colour is obtained in the hydrophobic hexane (Fig. 5a), whereas a right-handed helix with a reddish colour is formed in hydrophilic acetic acid solvent, as shown in Fig. 5b. The reddish colour is caused by Bragg diffraction from the opal structure and the bluish colour is from the scattering of uncorrelated dielectric silica spheres.[1] The local pitch length (p) and twisting power (θ, an angle between the helical axis and the twisted *y*-axis of the sample) of these helical actuators, which are related to the sensitivity of the actuating switch, are difficult to measure because the helices become irregular during a drying process due to the nature of uneven evaporation of the solvent. However, regular right- and left-handed helical structures with specific twisting powers can be obtained by confining the helical actuators in tubes. The handedness of the helical actuator is identical to that of the helical actuating switch in the solvent and the final dimensions of the helical structure in the tube permanently remain due to the geometric confinement. When a 3.5 mm diameter tube is used during the deswelling process, regular left-handed (Fig. 5c) and right-handed (Fig. 5d) helical opal structures are obtained with 70° and 73° twisting powers, respectively. These twisting powers decrease to 57° (Fig. 5e) and 62° (Fig. 5f) when the tubes are replaced with a larger diameter (4.5 mm) tube. The smaller the tube diameter with the steeper the triangular PDMS layer slope is, the larger the twisting power with the smaller the pitch length is. Therefore, the sensitivity of the switch can be tailored through the slope angle of the triangular PDMS layer and the diameter of the confining tube. These colour-tunable, reversible helical photonic actuators are more sensitive than the scrolled photonic actuators to environmental changes. It offers a way to use both the PDMS layer angle and the confining tube to precisely tune the response of the helical opal switch. After deswelling without

any confinement, both the right- and left-handed helical photonic sensors return to transparent planar structures.

A double twisted helical photonic actuator can be formed as shown in Fig. 3c and 6a. When a 2D colourless planar structure as shown in Fig. 2c is plunged into hexane solvent, the double twist structure is realized as shown in Fig. 6a. The double twist actuating behaviour is due to the competition of the twisting powers between the right-handed and the left-handed polypeptide-like helical structures. To prove this speculation, a right-handed and a left-handed helical structure are attached along the *yz*-plane by remaining the ends of the helical structure and then immersed in hexane solvent. The resulting photographic image is shown in Fig. 6b, which clearly reveals the competition between a right- and a left-handed twisting power. Furthermore, we simulate double twisting actuators by expanding the PDMS triangular regions, as shown in Fig. 7. Even though there is a range of value for the quantitative parameter, this computer simulation with finite element method (ABAQUS) helps us in understanding the double twisting actuators. Depending on the swelling ratio (V/V_0) of the PDMS layer, the helical angle with respect to double helical axis is measured and represented in Fig. 8. Even though the helical angles with respect to swelling ratios are functions of temperature, solvent, geometric dimensions and materials, these helical actuators can be used as chemical and biological sensors when the actuating devices are properly calibrated. For the application of sensors, the systematic approaches related to the stress distributions and the swelling ratios should be also conducted in the future.

In addition to the bending and twisting mechanisms, the folding mechanism can be used to fabricate sophisticated 3D objects. Folding, also known as "origami" technology, is the art of paper folding. Origami technology is already used in our everyday life and in advanced technology, such as paper-based milk container and solar cell panels for satellites. If the bending mechanism occurs on a continuous 2D surface, the folding mechanism can be considered as a 1D sharp bending. Based on this simple concept, a 2D structure can be programmed as schematically illustrated in Fig. 1c. Note that specific linear lines are consisted with bilayers of PDMS and PU70/HEMA30 and the last of surfaces is PU70/HEMA30 layer alone. Again, in order to secure the adhesion between PDMS and PU70/HEMA30, chemical bonds should be introduced as shown in Fig. 1c.

When the 2D structure described in Fig. 1c is submerged in hexane solvent, the PDMS layer will expand without any volume change of PU70/HEMA30 layers. By controlling the PDMS layer thickness with respect to the PU70/HEMA30 layer, this 2D programmed structure can be transformed to a 3D cubic object, as shown in Fig. 9a and b. The transformation behaviours of the 3D cubic object are also monitored with respect to time, as shown in Fig. 10. Since the speed of transformation is closely related to the diffusion of hexane solvent into the PDMS layer and the mechanical properties of PDMS and PU70/HEMA30 layers, the transformation time between the programmed 2D structure to the 3D object can be controlled by tuning the geometric dimensions of structures and the crosslinking density and interaction parameters of the materials used. When the 3D cubic object is deswollen, it reversibly returns back to the original 2D structure without observable damage. Yet, a much longer time is needed for this deswelling process. More precisely

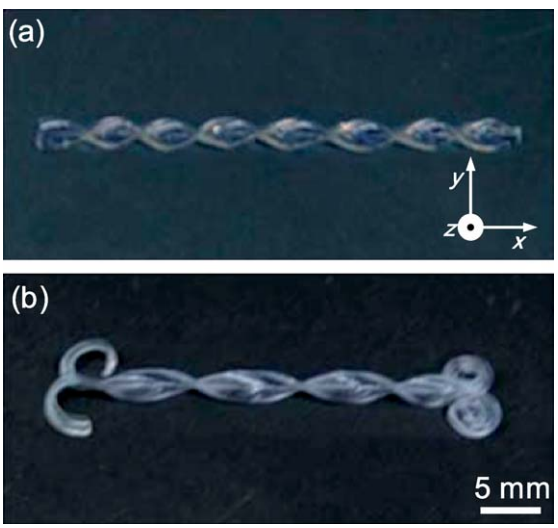

Fig. 6 (a) DNA-type double-twisting actuators taken after 120 s in hexane. Here, (b) is the photographic image of the DNA-type double-twisting actuators in hexane, which is fabricated by attaching a right-handed and a left-handed polypeptide-typed twisting actuators side by side.

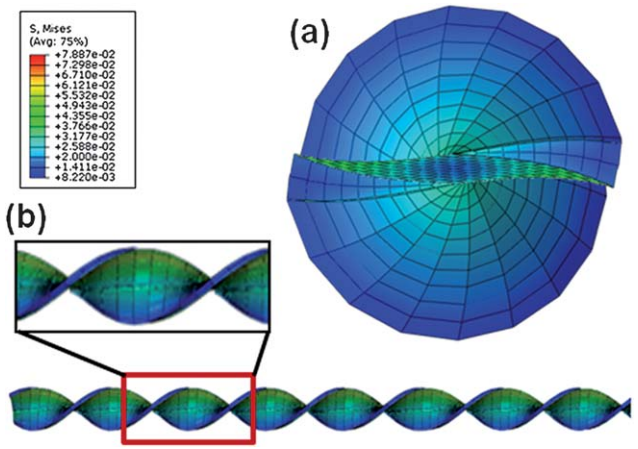

Fig. 7 Computer-simulated images of DNA-type twisting actuator: (a) end-on and (b) side-views. Here, red colour means a higher stress than blue colour.

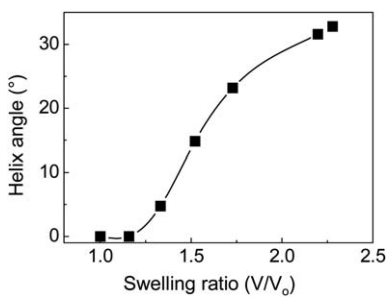

Fig. 8 Helical angle of DNA-type twisting actuator with respect to swelling ratio (V/V_0) of the PDMS layer.

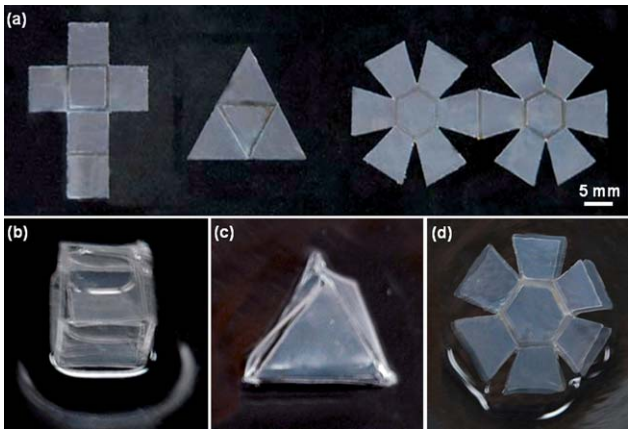

Fig. 9 (a) Programmed 2D structures, and their transformed 3D objects in hexane by folding mechanism: (b) cube, (c) pyramid, and (d) phlat ball.

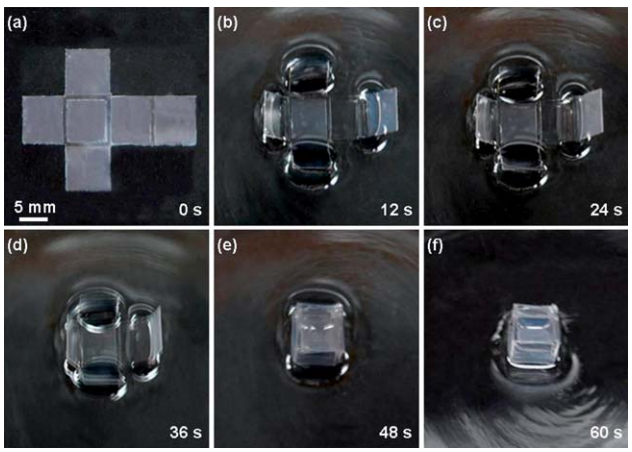

Fig. 10 Photographic images representing the transformation behaviours of the programmed 2D structure to the 3D cubic object *via* folding mechanism.

controlled actuating devices should be studied for obtaining the quantitative kinetic parameters of the swelling/deswelling processes. As shown in Fig. 9, pyramid and phlat ball objects are also able to be fabricated by transforming the 2D programmed structure.

Our results show that if the folding, bending and twisting mechanisms are properly applied, sophisticated structures can be fabricated. When the transformation mechanisms from the programmed 2D structures to the 3D objects reported here are combined with more elaborate technology such as nano-patterning or controlled drug release, this unique technique may be applied in the field of mechanical actuators, and optoelectronic and bio-mimetic devices.

Experimental

Materials and sample preparations

A transparent poly(dimethylsiloxane) (PDMS) (Dow Corning, Sylgard 184®) elastomer with a refractive index that matched that of silica was selected as the material for hydrophobic layer of the actuator. For the hydrophilic layer, a ultra-violet (UV)-curable elastomeric polyurethane (PU) precursor (Noland product, NOA 71) and a hydrogel 2-hydroxyethyl methacrylate (HEMA) monomer (Sigma Aldrich) with its 5 wt% darocur-1173 initiator (Chiba Co.) were blended in a series of compositions. We chose a hydrophilic transparent layer consisting of 70 wt% PU and 30 wt% HEMA (PU70/HEMA30) which is elastic and responds to hydrophilic solvents. The glass transition temperatures were measured utilizing both differential scanning calorimetry and dynamic mechanical analysis and the tensile properties of PU/HEMA layers at various compositions at room temperature are also evaluated to determine the appropriate content of HEMA in the PU/HEMA layer. To combine the multi-faceted environmental responsiveness of polymer gels with photonically active structures, silica colloidal FCC crystals (silica sphere diameter = 270 nm, Bangs Laboratories) were first assembled on the fluorinated silane (tridecafluoro-1,1,2,2-tetrahydrooctyltrichlorosilane, Sigma Aldrich) monolayer treated mold with dimensions of 2 mm × 40 mm × 0.2 mm. Utilizing Colvin's method multiple times, we controlled the thickness of the silica colloidal PC to be 0.08 ± 0.01 mm (~300 silica sphere layers). SEM images (Fig. 2a and b) show the FCC crystal structures of colloid crystals. The hydrophobic PDMS precursor infiltrated the silica colloidal template and was then thermally cured at 65 °C for 12 h. Before applying the hydrophilic PU70/HEMA30 layer, a methacryloxypropyltrimethyoxysilane (Sigma Aldrich) monolayer was created on the oxygen plasma treated PDMS as an adhesive between the hydrophobic PDMS and a hydrophilic PU/HEMA layer. In order to keep the sample thickness even, parafilm and a glass plate were placed on the top of the mold during the UV curing process of the hydrophilic PU70/HEMA30 layer. The final opal photonic crystal planar switches were peeled from the molds and stored in vacuum before carrying out characterization and analysis.

Equipment and experiments

The silica colloidal opal and the PDMS imbedded opal morphologies were investigated by SEM (JEOL 6060 and FESEM JSM-7401). The photographic images of photonic actuators were taken using a digital camera (EOS 5D, Canon). Utilizing oxygen plasma (PDC-32 G, HARRICK) for 4 min at 75 mTorr and 150 W, hydroxyl functions, which can react with methacryloxypropyltrimethoxysilane in ethanol, were created on the surface of the PDMS-embedded opals. Swelling tests and gel content measurements for PDMS and PU70/HEMA30 in hexane, acetic acid and ethyl acetate were carried out on samples with dimensions of 5 mm × 30 mm × 1 mm. Reflectivity spectra were obtained using an optical microscope (Zeiss Axioscop) equipped with a fiber-optic spectrometer (Stellarnet EPP2000) and a near infrared spectrometer (6000i, Varian) using a silver-coated metallic mirror as a 100% respective reference. A finite element method (FEM) analysis was performed using a commercially available FEM program (ABAQUS version 6.8, Dassault Systems, USA). The 8-node continuum shell elements (so-called SC8R) and the hyper-elastic material behaviour model provided from the company were used to simulate the structure. The stresses generated during the transformations were contoured on the surface of the deformed structures.

Conclusions

Reversible colour and shape tunable photonic actuators have been constructed by transforming the programmed 2D structures to the 3D objects *via* the bending, twisting and folding mechanisms. By changing geometrical factor, selected materials and polarity of the solvents, the shape and colour of the scrolled, helical and cubic actuators can be achieved. When the folding, bending and twisting technologies are combined with lithographic patterning technology in micrometre length scale, this unique technique may have a great potential for the applications in mechanical actuators, and optoelectronic and bio-mimetic devices.

Acknowledgements

This work was mainly supported by NRF-2010-0015277 and NSL-S1-08A01003210, Korea. J.-H. Jang thanks for the support from BRL program of NRF, Korea.

References

1 K.-U. Jeong, J.-H. Jang, C. Y. Koh, M. J. Graham, K.-Y. Jin, S.-J. Park, C. Nah, M.-H. Lee, S. Z. D. Cheng and E. L. Thomas, *J. Mater. Chem.*, 2009, **19**, 1956.

2 (*a*) H. Jeon, H. Hidai and D. J. Hwang, *J. Biomed. Mater. Res., Part A*, 2010, **93**, 56; (*b*) S. Y. Lin, J. G. Fleming, D. L. Hetherington, B. K. Smith, R. Biswas, K. M. Ho, M. M. Sigalas, W. Zubrzycki, S. R. Kurtz and J. Bur, *Nature*, 1998, **394**, 251; (*c*) H. J. Choi, K.-U. Jeong, L.-C. Chien and M.-H. Lee, *J. Mater. Chem.*, 2009, **19**, 7124; (*d*) L. Viry, C. Mercader, P. Miaudet, C. Zakri, A. Derre, A. Kuhn, M. Maugey and P. Poulin, *J. Mater. Chem.*, 2010, **20**, 3487; (*e*) S. Berhanu, F. Tariq, T. Jones and D. W. McComb, *J. Mater. Chem.*, 2010, **20**, 8005.

3 (*a*) J. H. Jang, C. K. Ullal, M. M. Maldovan, T. Gorishnyy, S. Kooi, C. Y. Koh and E. L. Thomas, *Adv. Funct. Mater.*, 2007, **16**, 3027; (*b*) B. H. Cumpston, S. P. Ananthavel, S. Barlow, D. L. Dyer, J. E. Ehrlich, L. L. Ersjine, A. A. Heikal, S. M. Kuebler, I.-Y. S. Lee, D. McCord-Maughon, J. Qin, H. Rockel, M. Rumi, X.-L. Wu, S. R. Marder, R. Seth and J. W. Perry, *Nature*, 1999, **398**, 51.

4 (*a*) G. M. Gratson, M. J. Xu and J. A. Lewis, *Nature*, 2004, **428**, 386; (*b*) M. Deubel, G. Von Freymann, M. Wegener, S. Pereira, K. Busch and C. M. Soukoulis, *Nat. Mater.*, 2004, **3**, 444; (*c*) S. Kawata, H. B. Sun, T. Tanaka and K. Takada, *Nature*, 2001, **412**, 697.

5 (*a*) P. Vukusic, J. R. Sambles and C. R. Lawrence, *Nature*, 2000, **404**, 457; (*b*) M. Maldovan and E. L. Thomas, *Nat. Mater.*, 2004, **3**, 593; (*c*) N. V. Dziomkina and G. J. Vancso, *Soft Matter*, 2005, **1**, 265; (*d*) A. Yethiraj, *Soft Matter*, 2007, **3**, 1099; (*e*) I. Musevic and M. Skarabot, *Soft Matter*, 2008, **4**, 195; (*f*) S. V. Ahir and E. M. Terentjev, *Nat. Mater.*, 2005, **4**, 491; (*g*) V. H. Ebron, J. W. Yang, D. J. Seyer, M. E. Kozlov, J. Y. Oh, H. Xie, J. Razal, L. J. Hall, J. P. Ferraris, A. G. MacDiarmid and R. H. Baughman, *Science*, 2006, **311**, 1580; (*h*) R. D. Rey, *Soft Matter*, 2007, **3**, 1349; (*i*) S. Haider, S. Y. Park and S. H. Lee, *Soft Matter*, 2008, **4**, 485; (*j*) P. D. Thornton, R. J. Mart, S. J. Webb and R. V. Ulijn, *Soft Matter*, 2008, **4**, 821; (*k*) S. F. Mason, *Nature*, 1984, **311**, 19; (*l*) C. Y. Li, S. Z. D. Cheng, J. J. Ge, F. Bai, J. Z. Zhang, I. K. Mann, F. W. Harris, L.-C. Chien, D. Yan, T. He and B. Lotz, *Phys. Rev. Lett.*, 1999, **83**, 4558; (*m*) C. Y. Li, S. Z. D. Cheng, X. Weng, J. J. Ge, F. Bai, J. Z. Zhang, B. H. Calhoun, F. W. Harris, L.-C. Chien and B. Lotz, *J. Am. Chem. Soc.*, 2001, **123**, 2462; (*n*) H. Shen, K.-U. Jeong, H. Xiong, M. J. Graham, S. Leng, J. X. Zheng, H. Huang, M. Guo, F. W. Harris and S. Z. D. Cheng, *Soft Matter*, 2006, **2**, 232; (*o*) R. J. Mart, R. D. Osborne, M. M. Stevens and R. V. Ulijn, *Soft Matter*, 2006, **2**, 822; (*p*) J. L. Gornall and E. M. Terentjev, *Soft Matter*, 2008, **4**, 544; (*q*) G. Zubay, *Biochemistry*, Macmillan Publishing Company, New York, 2nd edn, 1988, pp. 845–1151.

6 (*a*) J. Y. Huang, X. D. Wang and Z. L. Wang, *Nano Lett.*, 2006, **6**, 2325; (*b*) H. Stoyanov, M. Kollosche, M. Matthias, N. Denis and G. Kofod, *J. Mater. Chem.*, 2010, **20**, 7558.

7 J. D. Jonannopoulos, R. D. Meade and J. M. Winn, *Photonic Crystals*, Princeton University, 1995.

8 (*a*) J. H. Holtz and S. A. Asher, *Nature*, 1997, **389**, 829; (*b*) J. M. Weissman, H. B. Sunkara, A. S. Tse and S. A. Asher, *Science*, 1996, **274**, 959; (*c*) M. Fialkowski, A. Bitner and B. A. Grzybowski, *Nat. Mater.*, 2005, **4**, 93; (*d*) B. Lotz and S. Z. D. Cheng, *Polymer*, 2005, **46**(3), 577.

9 (*a*) R. D. Kamien, *Science*, 2007, **315**, 1083; (*b*) Y. Klein, E. Efrati and E. Sharon, *Science*, 2007, **315**, 1116; (*c*) Y. Osada, H. Okuzaki and H. Hori, *Nature*, 1992, **355**, 242; (*d*) E. Smela, *Adv. Mater.*, 2003, **15**, 481; (*e*) S. J. Kim, G. M. Spinks, S. Prosser, P. G. Whitten, G. G. Wallace and S. I. Kim, *Nat. Mater.*, 2006, **5**, 48.

10 K. J. Kim, W. Yim, J. W. Paquette and D. Kim, *J. Intell. Mater. Syst. Struct.*, 2007, **18**, 123.

11 (*a*) R. Nambudripad, M. Bansal and V. Sasisekharan, *Int. J. Pept. Protein Res.*, 1981, **18**, 374; (*b*) V. Sasisekharan and V. N. Balaji, *Macromolecules*, 1979, **12**, 28.

12 K.-U. Jeong, B. S. Knapp, J. J. Ge, S. Jin, M. J. raham, H. Xiong, F. W. Harris and S. Z. D. Cheng, *Macromolecules*, 2005, **38**, 8333.

13 (*a*) T. Otani, F. Araoka, K. Ishikawa and H. Takezoe, *J. Am. Chem. Soc.*, 2009, **131**, 12368; (*b*) F. Araoka, N. Y. Ha, Y. Kinoshita, B. Park, J. W. Wu and H. Takezoe, *Phys. Rev. Lett.*, 2005, **94**, 137801; (*c*) H. Koshima, M. Nagano and T. Asahi, *J. Am. Chem. Soc.*, 2005, **127**, 2455; (*d*) K. Maeda, K. Morino, Y. Okamoto, T. Sato and E. Yashima, *J. Am. Chem. Soc.*, 2004, **126**, 4329.

14 S. Cranford, D. Sen and M. J. Buehler, *Appl. Phys. Lett.*, 2009, **95**(12), 123121.

15 (*a*) J. S. Randhawa, L. V. Kanu, G. Singh and D. H. Gracias, *Langmuir*, 2010, **26**, 12534; (*b*) D. H. Gracias, M. Boncheva, O. Omoregie and G. M. Whitessides, *Appl. Phys. Lett.*, 2002, **80**, 2802; (*c*) D. H. Gracias, V. Kavthekar, J. C. Love, K. E. Paul and G. M. Whitesides, *Adv. Mater.*, 2002, **14**, 235.

16 (*a*) J.-H. Cho and D. H. Gracias, *Nano Lett.*, 2009, **9**, 4049; (*b*) J.-H. Cho, T. James and D. H. Gracias, *Adv. Mater.*, 2010, **22**, 2320.

17 (*a*) P. Jiang, J. F. Bertone, K. S. Hwang and V. L. Colvin, *Chem. Mater.*, 1999, **11**, 2132; (*b*) P. Jiang, K. S. Hwang, D. M. Mittleman, J. F. Bertone and V. L. Colvin, *J. Am. Chem. Soc.*, 1999, **121**, 11630.

